Available online at www.sciencedirect.com

SCIENCE DIRECT®

Journal of Molecular Catalysis A: Chemical 200 (2003) 291–300

JOURNAL OF MOLECULAR CATALYSIS A: CHEMICAL

www.elsevier.com/locate/molcata

Effect of promoter Ce on silver-molybdenum-phosphate catalysts for selective oxidation of propane to acrolein

Xin Zhang [a,*], Hui-lin Wan [b], Wei-zheng Weng [b], Xiao-dong Yi [b]

[a] *State Key Laboratory of C_1 Chemistry and Technology, Department of Chemistry, Tsinghua University, Beijing 100084, PR China*

[b] *State Key Laboratory of Physical Chemistry for Solid Surfaces, Department of Chemistry, Xiamen University, Xiamen 361005, PR China*

Received 28 June 2002; received in revised form 10 January 2003; accepted 13 January 2003

Abstract

A series of $Me_nAg_{0.3}Mo_{0.5}P_{0.3}O_y$ (Me = Cu, Zn, Mn, W, Ce, Pr, Nd) and $Ag_{0.3}Mo_{0.5}P_{0.3}O_x$ catalysts were prepared. The addition of Ce to $Ag_{0.3}Mo_{0.5}P_{0.3}O_x$ catalysts improved the catalytic performance in selective oxidation of propane to acrolein, and $Ce_{0.1}Ag_{0.3}Mo_{0.5}P_{0.3}O_x$ catalysts showed the highest acrolein selectivity (28.7%) and yield (4.4%). The physicochemical properties of $Ag_{0.3}Mo_{0.5}P_{0.3}O_x$ and $Ce_nAg_{0.3}Mo_{0.5}P_{0.3}O_x$ ($n = 0.1$–0.5) catalysts have been comparatively characterized by BET, XRD, H_2-TPR, XPS, EPR and C_3H_8(C_3H_6)-TPD. Significant differences in physicochemical properties between $Ag_{0.3}Mo_{0.5}P_{0.3}O_x$ and Ce doped $Ag_{0.3}Mo_{0.5}P_{0.3}O_x$ catalysts have been observed, which is due to the formation of the redox cycle ($Ce^{3+} + Mo^{6+} \Leftrightarrow Ce^{4+} + Mo^{5+}$) in the $Ce_nAg_{0.3}Mo_{0.5}P_{0.3}O_y$ catalyst. Such effect modified the reducibility, the concentration of Mo^{5+}, the activation of propane and the transformation of possible intermediate propene to acrolein, which in return greatly influenced the catalytic performance of Ce doped $Ag_{0.3}Mo_{0.5}P_{0.3}O_x$ catalysts in selective oxidation of propane to acrolein. The proper addition of Ce to $Ag_{0.3}Mo_{0.5}P_{0.3}O_x$ catalyst improved the acrolein selectivity and yield.

Keywords: Propane; Selective oxidation; Acrolein; Redox cycle

1. Introduction

The selective oxidation of light alkane to oxygenate is attractive because it is potential utilization of cheap row materials [1–3]. A great deal of research has already been done so far to achieve selective oxidation of propane to acrolein and/or acrylic acid by using multi-component oxide catalysts, which are based on vanadium and/or molybdenum [1–3]. The redox properties of catalysts always play important roles in activity and selectivity in selective oxidation of propane, because the selective oxidation of propane usually processes via Mars van Krevelen mechanism. It is well known that promoters could modify the redox properties of the catalysts, which in return determine the activity and selectivity in selective oxidation of propane.

The best catalyst for selective oxidation of propane to acrolein obtained up to now are BiMoVO multicompound catalysts with the Keggin structure developed by Moro-oka and coworkers [3–6]. They observed that the molybdenum component was necessary for good activity and selectivity to acrolein. The vanadium component improved propane conversion

* Corresponding author. Tel.: +86-10-6772592; fax: +86-10-62792122.
E-mail address: zhangxinzhangcn@yahoo.com.cn (X. Zhang).

1381-1169/03/$ – see front matter © 2003 Elsevier Science B.V. All rights reserved.
doi:10.1016/S1381-1169(03)00047-5

and the addition of Ag to BiMoVO significantly enhanced acrolein selectivity [3–6]; 65% acrolein selectivity with 13% propane conversion was obtained on the optimized $Ag_{0.01}Bi_{0.85}Mo_{0.54}V_{0.45}O_4$ catalysts [4]. Baerns et al. [7] reported that acrolein selectivity amounted to 34 and 20% (yield of 3.2 and 2.7%) when $Ag_{0.01}Bi_{0.85}Mo_{0.54}V_{0.45}O_4/Ca_7Bi_5Mo_{12}O_x$ and $Ag_{0.01}Bi_{0.85}Mo_{0.54}V_{0.45}O_4/Mg_7Bi_5Mo_{12}O_x$ catalysts were used, respectively. However, almost no acrolein was formed on $Ag_{0.01}Bi_{0.85}Mo_{0.54}V_{0.45}O_4/Me_xO_y$ ($Me_xO_y = Al_2O_3$, TiO_2, SiO_2) catalysts. The difference in catalytic performance could be due to oxygen species involved in selective oxidation of propane to acrolein, influencing the reaction mechanism. Teng and Kobayashi [8] observed that the addition of K^+ to the Fe/SiO_2 catalysts appreciably enhanced propane conversion along with high acrolein selectivity. Adjacency of Fe and K on the silica surface seemed to be important for the high oxygenate yield.

The most effective catalysts for propane oxidation to acrylic acid are Mo-V-Te-Nb-O catalysts reported by Ushikubo et al. [10], Lin [2] and Lin and Linsen [9,11,12]. The substitution of Sb for Te in the Mo-V-Te-Nb-O catalyst decreased propane conversion and acrylic acid selectivity but its overall performance is quite good [2]. Takahashi et al. [13] found that the addition of K to Mo-V-Sb-Nb-O improved propane conversion. Li et al. [14] reported that the $H_3PMo_{12}O_{40}$(Py) catalyst reduced by pyridine showed higher catalytic performance in propane oxidation to acrylic acid than the unreduced $H_3PMo_{12}O_{40}$ catalyst. The $H_3PMo_{12}O_{40}$(Py) catalyst is assumed to the highly restrain orthorhombic secondary structure against reoxidation, and Lewis acid site was generated with the formation of the primary oxygen-deficient Keggin structure.

VPO is another promising catalyst for selective oxidation of propane to arylic acid. A lot of works have been done about the effect of promoters on the catalytic performance and properties of VPO. Deng and coworkers [18,19] reported that the addition of Zr to the VPO catalyst could significantly enhanced acrylic acid selectivity. Cheng et al. [20] reported that 0.01 wt.% Ce doped VPO showed 18.8% yield acrylic acid, which is the highest acrylic acid yield reported on VPO catalysts so far. Wang et al. [21] investigated the influence of promoters (Co, Bi, Mo, Te, Nd, B) on the VPO catalyst. They observed that the addition of such promoters could not improve acrylic acid selectivity. In order to develop effective catalysts for selective oxidation of propane, systematic studies on the effects of promoters should be done.

In the present work, $Ag_{0.3}Mo_{0.5}P_{0.3}O_x$ and Me doped $Ag_{0.3}Mo_{0.5}P_{0.3}O_x$ (Me = Cu, Zn, W, Mn, Ce, Pr, Nd) catalysts were prepared. The performance of these catalysts in selective oxidation of propane to acrolein has been tested. The results show that the promoter Ce obviously enhanced propane conversion and acrolein selectivity. In order to clarify the role of promoter Ce, physicochemical properties of the Ce-doped and undoped catalysts such as the structure, the redox properties, the Mo^{6+}/Mo^{5+} ratio, and the interaction between propane and the catalysts have been comparatively characterized by BET, XRD, TPR, XPS, EPR and TPD technology, etc. and the transformation of possible intermediate propene to acrolein has been also investigated.

2. Experimental

2.1. Catalyst preparation

$Ag_{0.3}Mo_{0.5}P_{0.3}O_x$ (Ag/Mo/P = 0.3/0.5/0.3, mol ratio) catalyst and $Me_nAg_{0.3}Mo_{0.5}P_{0.3}O_x$ (Me/Ag/Mo/P = n/0.3/0.5/0.3, mol ratio, Me = Cu, Zn, W, Mn, Ce, Pr, Nd) catalysts were, respectively, prepared by the method of grinding $(NH_4)H_2PO_4$, MoO_3, Ag_2O and MeO_x powder (such as CeO_2, ZnO, CuO, etc.) with certain amount of deionized water. The samples were dried overnight in air at 383 K. After drying, the samples were calcinated at 623 K for 5 h and then at 823 K for 12 h.

2.2. Catalytic testing

The catalytic test was carried out at atmospheric pressure in a continuous flow system with a fixed bed quartz tubular reactor (i.d. = 6 mm). To minimize possible homogeneous reactions, the space of the reactor up and down the catalyst bed (0.5 g, 60–80 mesh) was filled with quartz wool. The exit gas were heated to 393 K to prevent products condensation. The feedstock and products were analyzed with two on-line gas chromatographs with three columns, TDX-601 column and

Al_2O_3 column impregnated with squalane (102-GC, TCD) for the separation of C_3H_8, C_3H_6, C_2H_4, C_2H_6, CO, CO_2, and GDX-103 column (103-GC FID) for the separation of acrolein, acetone and propanal, etc.

2.3. Characterization

The BET surface area of catalysts was measured by a ST-03 adsorptionmeter. The phase structures of the catalysts were identified by Rigaku Rotflex D/Max-C powder X-ray diffractometer (XRD) with Cu Kα (λ = 0.15046 nm).

Both the temperature-programmed reduction (TPR) experiments and the temperature-programmed desorption experiments (TPD) were carried out using a temperature-programmed reaction-mass spectrometer (Omnistar GSD 3000) instrument. In the TPR experiments, the sample (ca. 100 mg) was exposed to a 20 ml/min 5% H_2/N_2 flow, and heated at rate of 10 K/min. For the TPD experiments, the sample was pretreated in 20 ml/min propane (propene) flow for 30 min at room temperature (RT), and then He flow was switched to purge the gas phase propane (propene). The desorption was performed from RT to 923 K at a heating rate of 10 K/min.

The X-ray photoelectron spectroscopy (XPS) measurements were performed by VG ESCLAB MK-II spectrometer wit Al Kα (1486.6 eV, 10.1 kV). The spectra were referenced with respect to C 1s line at 284.7 eV. The measurement error is ±0.2 eV.

The electronic paramagnetic resonance (EPR) spectra were obtained by a Brucker 200D-SCR spectrometer at RT. The klystron frequency was 9.6 GHz and magnetic field modulation was 100 KHz.

3. Results

3.1. Catalytic performance

3.1.1. Propane oxidation

The performance of the catalysts in selective oxidation of propane to acrolein is shown in Table 1. The blank reactor did not show activity in oxidation of propane, indicating that the homogeneous reaction could not make significant contribution to the heterogeneous oxidation of propane under our experiment conditions. $Ag_{0.3}Mo_{0.5}P_{0.3}O_x$ catalyst showed 5.6% acrolein selectivity and 67.9% propene selectivity with 10.9% propane conversion. The addition of promoter such as Cu, Zn, W, Mn, Ce, Pr, Nd to $Ag_{0.3}Mo_{0.5}P_{0.3}O_x$ catalysts changed catalytic activity and products distribution in selective oxidation of propane. In all the investigated catalysts, Ce doped $Ag_{0.3}Mo_{0.5}P_{0.3}O_x$ catalysts showed higher propane conversion and higher acrolein selectivity. In the case of Ce doped $Ag_{0.3}Mo_{0.5}P_{0.3}O_x$ catalysts, propane conversion and products distribution depended on the Ce-content. With the Ce-content increasing, propane conversion increased; acrolein selectivity firstly

Table 1
Catalytic performance of these catalysts for selective oxidation of propane to acrolein

Catalysts	Conversion of C_3H_8 (%)	Selectivity (%)					Yield (%)
		C_3H_6	ACR	PA + AT	C_2	CO_x	ACR
$Ag_{0.3}Mo_{0.5}P_{0.3}O_x$	10.9	67.9	5.6	4.8	2.8	18.5	0.6
$Cu_{0.1}Ag_{0.3}Mo_{0.5}P_{0.3}O_x$	11.6	24.9	Tr	8.8	27.7	38.6	–
$Zn_{0.1}Ag_{0.3}Mo_{0.5}P_{0.3}O_x$	10.2	45.2	6.0	8.0	5.3	35.5	0.6
$Mn_{0.1}Ag_{0.3}Mo_{0.5}P_{0.3}O_x$	5.3	45.3	–	–	7.6	47.1	–
$W_{0.1}Ag_{0.3}Mo_{0.5}P_{0.3}O_x$	12.6	37.2	–	–	25.3	37.5	–
$Pr_{0.1}Ag_{0.3}Mo_{0.5}P_{0.3}O_x$	12.8	66.9	3.9	–	4.3	24.9	0.5
$Nd_{0.1}Ag_{0.3}Mo_{0.5}P_{0.3}O_x$	8.8	38.2	–	–	21.5	40.3	–
$Ce_{0.05}Ag_{0.3}Mo_{0.5}P_{0.3}O_x$	13.2	43.2	7.0	2.0	20.4	27.4	0.9
$Ce_{0.1}Ag_{0.3}Mo_{0.5}P_{0.3}O_x$	15.3	25.7	28.7	2.0	17.5	26.0	4.4
$Ce_{0.3}Ag_{0.3}Mo_{0.5}P_{0.3}O_x$	18.5	26.3	20.6	8.8	1.0	42.6	3.8
$Ce_{0.5}Ag_{0.3}Mo_{0.5}P_{0.3}O_x$	22.0	23.7	14.7	8.0	2.3	50.4	3.2

Reaction conditions: 773 K, $C_3H_8/O_2/N_2$ = 3/1/4, 2400 ml/(g cat h), atmospheric pressure. ACR: acrolein; PA + AT: propionaldehyde and acetone; C_2: C_2H_6, C_2H_4 and acetaldehyde; CO_x: CO and CO_2.

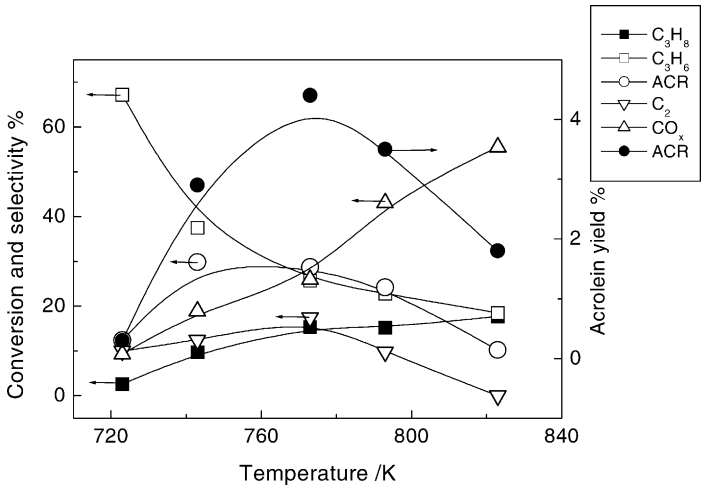

Fig. 1. Effect of reaction temperature on the catalytic performance in selective oxidation of propane to acrolein over $Ce_{0.1}Ag_{0.3}Mo_{0.5}P_{0.3}O_y$ catalyst. ACR: acrolein; C_2: C_2H_6, C_2H_4 and acetaldehyde; CO_x: CO_2 and CO.

increased and simultaneously propene selectivity decreased and CO_x selectivity increased. The maximal 4.4% acrolein yield with 28.7% acroelin selectivity was obtained on $Ce_{0.1}Ag_{0.3}Mo_{0.5}P_{0.3}O_y$.

The reaction temperature had great influence on propane conversion and products distribution of the $Ce_{0.1}Ag_{0.3}Mo_{0.5}P_{0.3}O_y$ catalyst in selective oxidation of propane to acrolein (Fig. 1). When the reaction temperature was elevated, propane conversion increased. The maximal acrolein selectivity and yield were observed with the rising of reaction temperature, while propene selectivity monotonically decreased. Deep oxidation products CO_x became favorable at the high temperatures.

The effect of space velocity on the catalytic performance of $Ce_{0.1}Ag_{0.3}Mo_{0.5}P_{0.3}O_y$ catalyst in selective oxidation of propane was also investigated. As can be seen in Fig. 2, propane conversion and products distribution varied as a function of space velocity. With the increase in space velocity, propane conversion

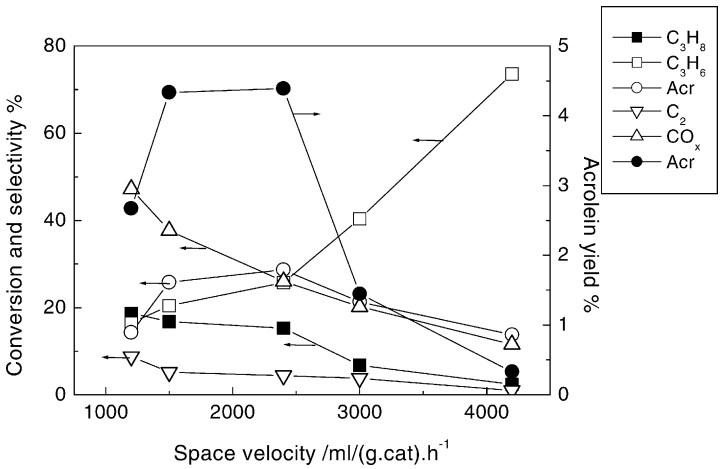

Fig. 2. Effect of space velocity on the catalytic performance in selective oxidation of propane to acrolein over $Ce_{0.1}Ag_{0.3}Mo_{0.5}P_{0.3}O_y$ catalyst. ACR: acrolein; C_2: C_2H_6, C_2H_4 and acetaldehyde; CO_x: CO_2 and CO.

decreased, while propene selectivity monotonously increased and acroelin selectivity gave maximal value at the space velocity of 2400 ml/(g cat h). In addition, the decrease of CO_x selectivity was observed with increasing space velocity.

These $Ce_nAg_{0.3}Mo_{0.5}P_{0.3}O_y$ catalysts showed good performance for acrolein formation in selective oxidation of propane. This work thus focuses on these catalysts.

3.1.2. Propene oxidation

It is well known that the primary products of a given reaction can be discriminated from high-order products by extrapolating products selectivity to zero conversion. Primary products have non-zero intercepts, while secondary and high-order products have zero intercepts [15]. In the case of selective oxidation of propane over $Ce_nAg_{0.3}Mo_{0.5}P_{0.3}O_y$ catalysts (Fig. 2), it is clear that the dominant primary products was propene because propene selectivity gradually increased with the decrease in propane conversion.

Table 2 shows that the results of propene oxidation over $Ag_{0.3}Mo_{0.5}P_{0.3}O_x$ and $Ce_nAg_{0.3}Mo_{0.5}P_{0.3}O_y$ catalysts. Acrolein and CO_x were main products in propene oxidation. The addition of Ce enhanced propene conversion and acrolein yield. Compared with $Ag_{0.3}Mo_{0.5}P_{0.3}O_x$ catalyst, acrolein selectivity was higher on $Ce_nAg_{0.3}Mo_{0.5}P_{0.3}O_y$ catalysts when the Ce/Mo ratio was varied from 0.05 to 0.3; however, it became lower as the Ce/Mo ratio increased to 0.5. In the case of $Ce_nAg_{0.3}Mo_{0.5}P_{0.3}O_x$ catalysts, the maximal acrolein selectivity and yield were observed on $Ce_{0.1}Ag_{0.3}Mo_{0.5}P_{0.3}O_x$ catalyst, and acrolein selectivity and yield monotonously decreased when the Ce/Mo ratio increased. An increase in CO_x selectivity was observed with the Ce-content. It can be noted that propene conversion almost kept constant as the Ce/Mo ratio increased from 0.1 to 0.5, which might be due to the total consumption of O_2 taking place.

By combining the propane oxidation and propene oxidation data, propene was primary product that was then oxidized to acrolein over these catalysts in selective oxidation of propane. The proper addition of Ce in the catalysts enhanced the conversion of propene to acrolein, but the oxidation of propene to deep oxidation products CO_x was favorable on the catalysts with Ce/Mo = 0.5.

3.2. Characterization

3.2.1. BET surface area and XRD characterization

The BET surface area of these catalysts is shown in Table 3. $Ag_{0.3}Mo_{0.5}P_{0.3}O_x$ had the lowest surface area of 10.6 m^2/g. The surface area of $Ce_nAg_{0.3}Mo_{0.5}P_{0.3}O_y$ catalysts was higher than that of $Ag_{0.3}Mo_{0.5}P_{0.3}O_x$, and slightly increased with increasing Ce-content.

The XRD patterns of $Ce_nAg_{0.3}Mo_{0.5}P_{0.3}O_y$ and $Ag_{0.3}Mo_{0.5}P_{0.3}O_x$ catalysts are shown in Fig. 3. MoO_3 and $AgMoO_2PO_4$ were main phases in $Ag_{0.3}Mo_{0.5}P_{0.3}O_x$ catalysts. In the case of $Ce_nAg_{0.3}Mo_{0.5}P_{0.3}O_y$ catalysts, new phases $CeMoO_6$ and CeO_2 were found. In addition, it can be noted that the peak intensities of $CeMoO_6$ and CeO_2 increased with increasing Ce-content, indicating that the amount of $CeMoO_6$ and CeO_2 increased.

3.2.2. TPR characterization

The TPR profiles of $Ce_nAg_{0.3}Mo_{0.5}P_{0.3}O_y$ catalysts, $Ag_{0.3}Mo_{0.5}P_{0.3}O_x$ catalyst, pure MoO_3 and

Table 2
Catalytic performances of these catalysts in selective oxidation of propene to acrolein

Catalysts	Conversion of C_3H_8 (%)	Selectivity (%)					Yield (%)
		ACR	PA	AT	C_2	CO_x	ACR
$Ag_{0.3}Mo_{0.5}P_{0.3}O_x$	16.6	24.9	5.6	5.6	31.4	32.5	4.1
$Ce_{0.05}Ag_{0.3}Mo_{0.5}P_{0.3}O_x$	21.0	26.8	7.8	2.9	32.5	30.0	5.6
$Ce_{0.1}Ag_{0.3}Mo_{0.5}P_{0.3}O_x$	34.3	34.8	1.8	1.8	6.2	55.2	11.9
$Ce_{0.3}Ag_{0.3}Mo_{0.5}P_{0.3}O_x$	36.5	31.6	5.3	1.6	7.4	54.1	11.5
$Ce_{0.5}Ag_{0.3}Mo_{0.5}P_{0.3}O_x$	36.1	15.1	2.7	1.5	18.5	62.2	5.4

Reaction conditions: 773 K, $C_3H_6/O_2/N_2$ = 3/1/4, 2400 ml/(g cat h), atmospheric pressure. ACR: acrolein; PA: propionaldehyde; AT: acetone; C_2: C_2H_6, C_2H_4, and acetaldehyde; CO_x: CO and CO_2.

Table 3
Physicochemical properties of $(Ce_n)Ag_{0.3}Mo_{0.5}P_{0.3}O_y$ catalysts

Catalysts	BET area (g/m^2)	Surface composition by XPS			Relative concentration of Mo^{5+} by EPR (a.u.)
		Ag/Mo	Ce/Mo	P/Mo	
$Ag_{0.3}Mo_{0.5}P_{0.3}O_x$	10.6	0.36	–	0.33	21.9
$Ce_{0.1}Ag_{0.3}Mo_{0.5}P_{0.3}O_x$	15.7	0.42	0.33	0.34	38.4
$Ce_{0.3}Ag_{0.3}Mo_{0.5}P_{0.3}O_x$	16.3	0.44	0.45	0.36	46.2
$Ce_{0.5}Ag_{0.3}Mo_{0.5}P_{0.3}O_x$	18.8	0.50	0.55	0.36	55.4

pure CeO_2 are presented in Fig. 4. The TPR profile of pure MoO_3 showed two reduction peaks at 926 and 1042 K, corresponding to the step-wise reduction of $Mo^{6+} \Rightarrow Mo^{4+}$ and $Mo^{4+} \Rightarrow Mo^0$, respectively [22,23]. CeO_2 showed two reduction peaks at ca. 811 and 1035 K with respect to the reduction of $Ce^{4+} \Rightarrow Ce^{3+} \Rightarrow Ce^0$ [24]. $Ce_nAg_{0.3}Mo_{0.5}P_{0.3}O_y$ catalysts and $Ag_{0.3}Mo_{0.5}P_{0.3}O_x$ catalysts exhibited the low temperature reduce peak (<500 K) and the high temperature reduce peaks (>700 K). The low temperature reduction peak near 420 K may be due to the reduction of $Ag^+ \Rightarrow Ag^0$ [25]. The high temperature reduction peaks could be assigned to the contributions of the reduction of Mo- and Ce-oxides. The reduction peaks (>700 K) shifted to the lower temperature when Ce was added to $Ag_{0.3}Mo_{0.5}P_{0.3}O_y$ catalysts, and they monotonically shifted toward the lower temperature with increasing Ce-content.

In order to estimate the H_2 consumption, the area of TPR profile was integrated. The H_2 consumption increased in the sequence $Ag_{0.3}Mo_{0.5}P_{0.3}O_y$ < $Ce_{0.1}Ag_{0.3}Mo_{0.5}P_{0.3}O_y$ < $Ce_{0.3}Ag_{0.3}Mo_{0.5}P_{0.3}O_y$ < $Ce_{0.5}Ag_{0.3}Mo_{0.5}P_{0.3}O_y$ catalyst. The results reveal that the reducibility of $(Ce_n)Ag_{0.3}Mo_{0.5}P_{0.3}O_y$ catalysts improved with increasing Ce-content.

3.2.3. EPR characterization

The EPR spectroscopy was used to investigate the presence and change of Mo^{5+} and Ce^{3+} in these catalysts (Fig. 5). The spectra of the catalysts exhibited signals with $g_1 = 1.94$ and $g_2 = 1.89$ attributed to Mo^{5+} [26,27]. No hyperfine structure due to Mo^{5+} ($S = 1/2$, $I = 5/2$) was observed, indicating that Mo^{5+} was not sufficiently apart from one another and the Mo^{5+} strong interaction had eliminated the hyperfine structure. The EPR signal at $g_3 = 1.98$ due to Ce^{3+} was also found in $Ce_nAg_{0.3}Mo_{0.5}P_{0.3}O_y$ catalysts [28,29].

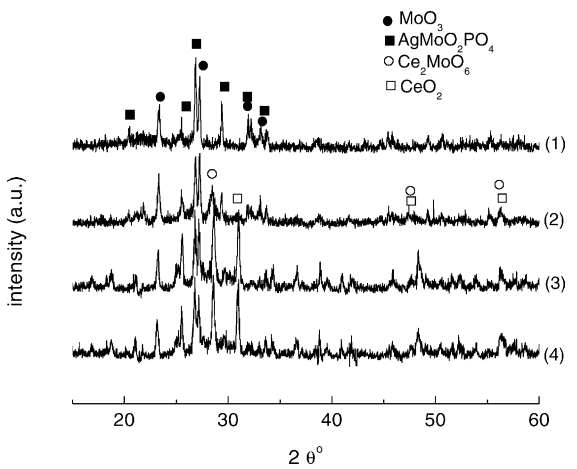

Fig. 3. XRD pattern of catalysts: (1) $Ag_{0.3}Mo_{0.5}P_{0.3}O_x$; (2) $Ce_{0.1}Ag_{0.3}Mo_{0.5}P_{0.3}O_y$; (3) $Ce_{0.3}Ag_{0.3}Mo_{0.5}P_{0.3}O_y$; (4) $Ce_{0.5}Ag_{0.3}Mo_{0.5}P_{0.3}O_y$.

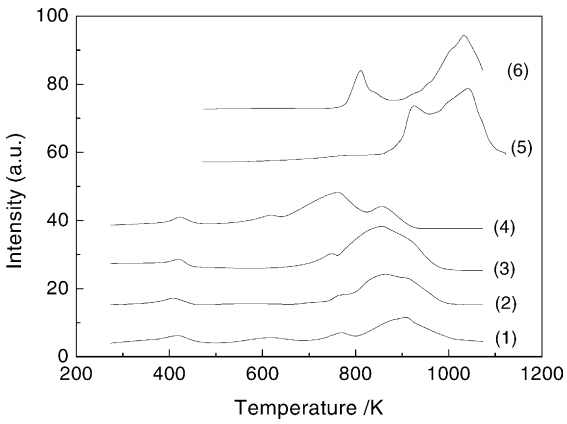

Fig. 4. H_2-TPR profiles of catalysts: (1) $Ag_{0.3}Mo_{0.5}P_{0.3}O_x$; (2) $Ce_{0.1}Ag_{0.3}Mo_{0.5}P_{0.3}O_y$; (3) $Ce_{0.3}Ag_{0.3}Mo_{0.5}P_{0.3}O_y$; (4) $Ce_{0.5}Ag_{0.3}Mo_{0.5}P_{0.3}O_y$; (5) MoO_3; (6) CeO_2.

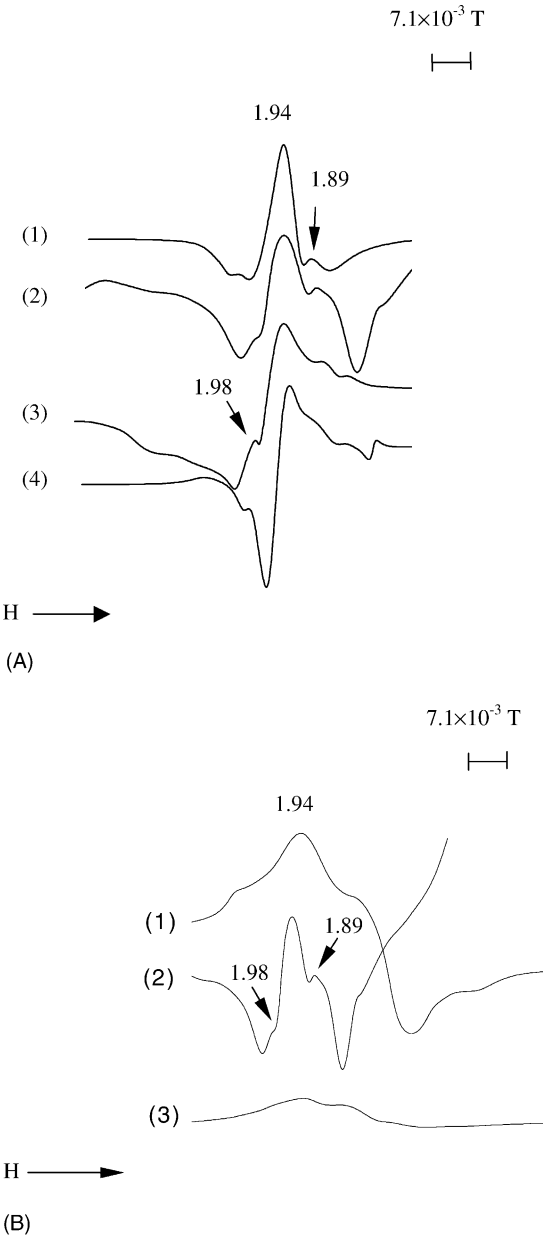

Fig. 5. (A) EPR spectra of catalysts: (1) $Ag_{0.3}Mo_{0.5}P_{0.3}O_x$; (2) $Ce_{0.1}Ag_{0.3}Mo_{0.5}P_{0.3}O_y$; (3) $Ce_{0.3}Ag_{0.3}Mo_{0.5}P_{0.3}O_y$; (4) $Ce_{0.5}Ag_{0.3}Mo_{0.5}P_{0.3}O_y$. (B) EPR spectra of $Ce_{0.1}Ag_{0.3}Mo_{0.5}P_{0.3}O_y$ catalyst treated under different conditions: (1) used catalysts; (2) fresh catalysts; (3) the catalysts treated with O_2 flow at 773 K for 15 min and then cooled to room temperature in N_2 flow.

The formulate $[I_i(\Delta H_{pp})_i^2]/[I(\Delta H_{pp})^2]_{standard\ sample}$ could be used to roughly estimate relative concentration of Mo^{5+} in the catalysts, in which I_i is intensity of peaks and ΔH_{pp} the line width at peak to peak maximum [32–35]. The results are shown in Table 3. The relative concentration of Mo^{5+} increased following the order of $Ag_{0.3}Mo_{0.5}P_{0.3}O_y$ < $Ce_{0.1}Ag_{0.3}Mo_{0.5}P_{0.3}O_y$ < $Ce_{0.3}Ag_{0.3}Mo_{0.5}P_{0.3}O_y$ < $Ce_{0.5}Ag_{0.3}Mo_{0.5}P_{0.3}O_y$ catalyst.

Fig. 5B gives the EPR spectra of $Ce_{0.1}Ag_{0.3}Mo_{0.5}P_{0.3}O_y$ treated under different conditions. Compared with the fresh catalyst, the EPR spectrum of the used catalyst showed broad and strong peak. After the catalyst was treated in O_2 flow at 773 K for 15 min and then sealed in a glass tube, the intensity of Mo^{5+} remarkably reduced. The results suggest that Mo^{5+}/Mo^{6+} and Ce^{3+}/Ce^{4+} were involved in the activation of molecular oxygen and oxidation of propane.

3.2.4. XPS characterization

In this study, oxidation state and relative surface concentration of composition have been investigated by using XPS. The XPS spectra of pure MoO_3 are used to identify the possible change of the state of Mo. The binding energy (BE) of Mo $3d_{5/2}$ on MoO_3 is 233.5 eV. The BE of Mo $3d_{5/2}$ on $Ag_{0.3}Mo_{0.5}P_{0.3}O_x$ was about 233.1 eV (Fig. 6). $Ce_nAg_{0.3}Mo_{0.5}P_{0.3}O_y$ catalysts showed the lower BE of Mo $3d_{5/2}$ than $Ag_{0.3}Mo_{0.5}P_{0.3}O_x$ catalyst. The BE of Mo $3d_{5/2}$ on $Ce_nAg_{0.3}Mo_{0.5}P_{0.3}O_y$ decreased from 232.8 to 232.5 eV with increasing Ce-content, suggesting that the electronic density around Mo nucleus increased, in other words, the coordinatively unsaturated Mo increased on the surface. In addition, shoulder peaks near 234.5 eV were observed, which may be assigned to Mo^{5+} $3d_{3/2}$.

Fig. 6 also gives Ce 3d XPS spectra on $Ce_nAg_{0.3}Mo_{0.5}P_{0.3}O_y$ catalysts. The peaks near 915.6 and 910.5 eV were assigned to Ce^{4+} [16,17]. The peak at 885.0 eV was due to Ce^{3+} [16,17]. With increasing Ce-content, the BE of Ce slightly fluctuated.

The value corresponding to relative surface concentration is presented in Table 3. Surface concentration was heavily dependent on the Ce-content in the catalysts. In the case of $Ce_nAg_{0.3}Mo_{0.5}P_{0.3}O_y$ catalysts, we note an increase in Ag and Ce concentrations, respectively, with increasing Ce-content. In addition in,

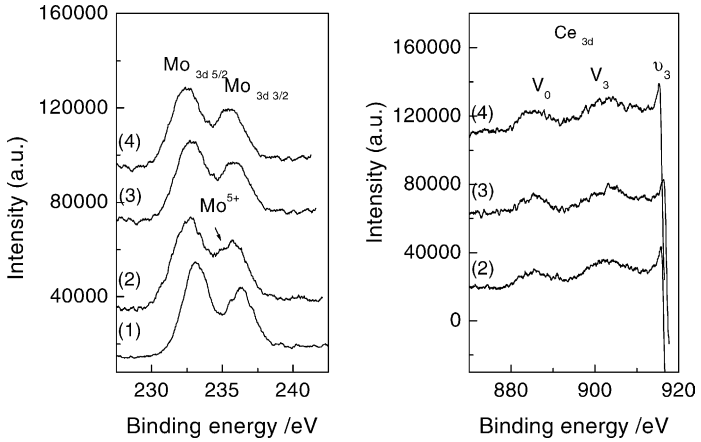

Fig. 6. XPS spectra of catalysts: (1) $Ag_{0.3}Mo_{0.5}P_{0.3}O_x$; (2) $Ce_{0.1}Ag_{0.3}Mo_{0.5}P_{0.3}O_y$; (3) $Ce_{0.3}Ag_{0.3}Mo_{0.5}P_{0.3}O_y$; (4) $Ce_{0.5}Ag_{0.3}Mo_{0.5}P_{0.3}O_y$.

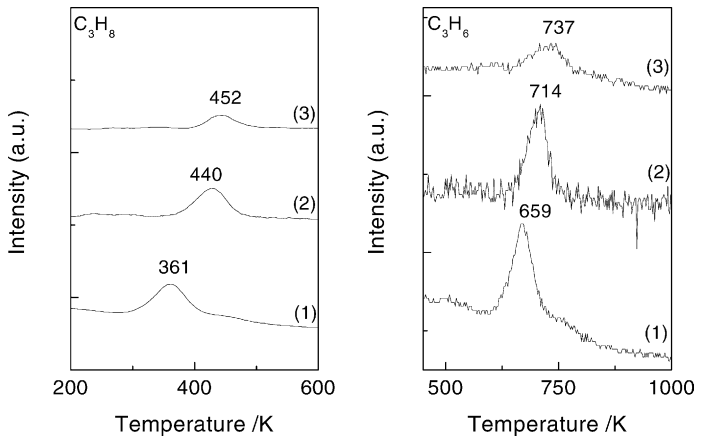

Fig. 7. TPD profiles of catalysts: (1) $Ag_{0.3}Mo_{0.5}P_{0.3}O_x$; (2) $Ce_{0.1}Ag_{0.3}Mo_{0.5}P_{0.3}O_x$; (3) $Ce_{0.5}Ag_{0.3}Mo_{0.5}P_{0.3}O_x$.

the ratio of Ag/Mo on $Ce_nAg_{0.3}Mo_{0.5}P_{0.3}O_y$ catalysts was higher than that on $Ag_{0.3}Mo_{0.5}P_{0.3}O_x$.

3.2.5. C_3H_8-TPD and C_3H_6-TPD characterization

In order to investigate the interaction between C_3H_8(C_3H_6) and the catalysts, the temperature-programmed desorption (TPD) experiments were carried out. The TPD profiles are shown in Fig. 7. C_3H_8-TPD profiles showed one desorption peak on both Ce doped $Ag_{0.3}Mo_{0.5}P_{0.3}O_y$ and undoped $Ag_{0.3}Mo_{0.5}P_{0.3}O_x$ catalyst, indicating that there was one kind of active sites for C_3H_8 adsorption on these catalysts. Compared with $Ag_{0.3}Mo_{0.5}P_{0.3}O_x$, the desorption peak shifted toward the higher temperature on Ce doped $Ag_{0.3}Mo_{0.5}P_{0.3}O_x$ catalysts. The results suggest that the addition of Ce enhanced the interaction between C_3H_8 and the catalysts. In the case of C_3H_6 desorption, one peak due to C_3H_6 desorption was observed on both Ce doped $Ag_{0.3}Mo_{0.5}P_{0.3}O_x$ and $Ag_{0.3}Mo_{0.5}P_{0.3}O_x$ catalysts. The desorption peak temperature shifted to higher temperature with the increase in the Ce-content, indicating that the promoter Ce enhanced C_3H_6 adsorption.

4. Discussion

The addition of promoter Ce in the catalysts modified the physicochemical properties, which in turn influenced the catalytic performance in selective

oxidation of propane to acroelin. The significant difference in physicochemical properties among the catalysts has been observed. The promoter Ce improved the reducibility, increased the relative concentration of Mo^{5+}, modified the surface composition, and enhanced the $C_3H_8(C_3H_6)$ adsorption on the catalysts. $Ce_nAg_{0.3}Mo_{0.5}P_{0.3}O_y$ catalysts had higher catalytic performance in selective oxidation of propane to acrolein than $Ag_{0.3}Mo_{0.5}P_{0.3}O_x$ catalyst. $Ce_{0.1}Ag_{0.3}Mo_{0.5}P_{0.3}O_y$ showed the highest 4.4% acrolein yield with 28.7% acroelin selectivity. In addition, the proper addition of Ce could enhance the transformation of possible intermediate propene to acrolein.

The variation of such properties of $Ce_nAg_{0.3}Mo_{0.5}P_{0.3}O_y$ catalysts could be due to the interaction between Mo and Ce in $Ce_nAg_{0.3}Mo_{0.5}P_{0.3}O_y$ catalysts. Both Mo^{5+} and Ce^{3+} were detected on $Ce_nAg_{0.3}Mo_{0.5}P_{0.3}O_y$ catalysts. The redox potential of Mo^{6+}/Mo^{5+} and Ce^{4+}/Ce^{3+} is about 0.3 eV, and −1.61 eV, respectively. Both Ce and Mo are able to activate/store oxygen and transform/release oxygen species. Hence, the redox cycle ($Ce^{3+} + Mo^{6+} \Leftrightarrow Ce^{4+} + Mo^{5+}$) can exist, improving the transfer of electron and oxygen species. With the increase in the Ce-content, the relative concentration of Mo^{5+} gradually increased, the lattice oxygen deficient sites around the coordinatively unsaturated Mo ion enhanced [14]. The more the lattice oxygen deficient sites, the easier the diffusion of oxygen [30,31]. Thus, the reducibility of the catalysts improved with the increase in the Ce-content.

In order to elucidate such changes to be responsible for the catalytic performance of Ce doped $Ag_{0.3}Mo_{0.5}P_{0.3}O_x$ catalysts, several methods have been employed. The catalytic performance has been identified in terms of specific activity (specific activity = mol propane converted ($m^2\,s^{-1}$)) and specific yield (specific selectivity = mol acrolein obtained ($m^2\,s^{-1}$)). The relationships of Ce-content with the reducibility and the concentration of Mo^{5+} and catalytic performance are presented in Figs. 8 and 9, respectively. A clear correlation was observed between the catalytic performance and physicochemical properties. With the increase in Ce/Mo ratio in these catalysts, the Mo^{5+} concentration gradually increased. The specific activity monotonously increased with the Mo^{5+} concentration; the acrolein specific

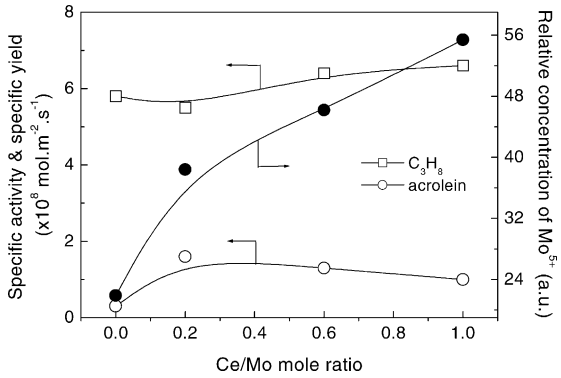

Fig. 8. Relationship of the Mo^{5+} concentration with the catalytic performance.

yield showed a volcano shape curve and gave the maximal value on the $Ce_{0.1}Ag_{0.3}Mo_{0.5}P_{0.3}O_y$ catalysts (Fig. 8). Likewise, an increase in H_2 consumption was observed with increasing Ce-content, and specific activity increased and the maximal acrolein specific yield was achieved on the $Ce_{0.1}Ag_{0.3}Mo_{0.5}P_{0.3}O_y$ catalysts (Fig. 9).

In selective oxidation of propane to acrolein on $Ce_nAg_{0.3}Mo_{0.5}P_{0.3}O_y$ catalysts, the oxygen deficient site around coordinatively unsaturated Mo^{5+} reacted with molecular oxygen to form lattice oxygen species that are active species for propane activation; simultaneously, the coordinatively unsaturated Mo^{5+} was oxidized to Mo^{6+} (Mars van Krevelen redox mechanism) [3]. The enhancement of reducibility is in favor of this process. Therefore, the more the concentration

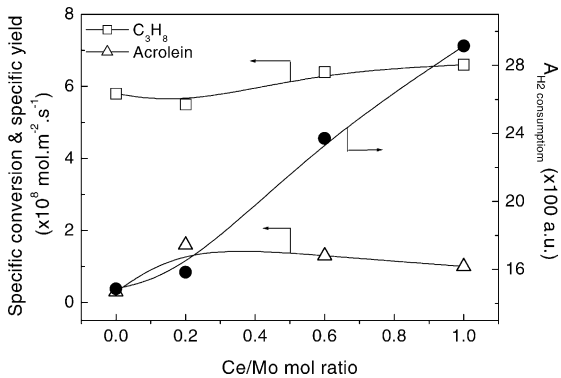

Fig. 9. Relationship of the H_2 consumption with the catalytic performance.

of Mo^{5+} and the stronger reducibility are, the higher the specific activity.

On the other hand, propene was the intermediate for the formation of acrolein in selective oxidation of peopane. The transformation of propene to acrolein will be mostly determined by the interaction of propene with the catalyst surface. As can be seen in Sections 3.2.5 and 3.1.2, the proper addition of Ce to the catalysts resulted in the enhancement of propene adsorption and transformation of propene to acroelin. Therefore, high acroelin selectivity and yield were obtained on $Ce_{0.1}Ag_{0.3}Mo_{0.5}P_{0.3}O_y$ catalyst. However, owing to much stronger interaction between propene and the $Ce_{0.5}Ag_{0.3}Mo_{0.5}P_{0.3}O_y$ catalyst, and the higher reducibility, intermediate propene could easily suffer deep oxidation to CO_x. Consequently, acrolein selectivity and yield was decreased on the $Ce_{0.5}Ag_{0.3}Mo_{0.5}P_{0.3}O_y$ catalyst in selective oxidation of propane.

5. Conclusions

In conclusion, the addition of promoter Ce to $Ag_{0.3}Mo_{0.5}P_{0.3}O_x$ modified the physicochemical properties such as the reducibility, the concentration of Mo^{5+}, surface composition, the propane adsorption as well as the transformation of intermediate propene to acrolein, which in turn determined the catalytic performance of these catalysts in selective oxidation of propane to acrolein. The maximal acrolein selectivity and yield were obtained on the $Ce_{0.1}Ag_{0.3}Mo_{0.5}P_{0.3}O_y$ catalyst. The formation of redox cycle ($Ce^{3+} + Mo^{6+} \Leftrightarrow Ce^{4+} + Mo^{5+}$) in $Ce_nAg_{0.3}Mo_{0.5}P_{0.3}O_y$ catalysts accounts for the change of physicochemical properties and performance of these catalysts.

Acknowledgements

This work is supported by the Ministry of Science and Technology (G1999022408).

References

[1] F. Cavani, F. Trifiro, Appl. Catal. A. 88 (1992) 115.
[2] M.M. Lin, Appl. Catal. A. 207 (2000) 1.
[3] M.M. Bettahar, G. Constentin, L. Savary, Appl. Catal. A. 145 (1996) 1.
[4] Y.C. Kim, W. Ueda, Y. Moro-oka, Appl. Catal. A. 70 (1991) 175.
[5] Y.C. Kim, W. Ueda, Y. Moro-oka, Stud. Surf. Sci. Catal. 50 (1990) 491.
[6] Y.C. Kim, W. Ueda, Y. Moro-oka, Catal. Today 13 (1992) 673.
[7] M. Barens, O.V. Buyevskaya, M. Kubik, Catal. Today 33 (1997) 85.
[8] Y. Teng, T. Kobayashi, Catal. Lett. 55 (1998) 33.
[9] W. Ueda, K. Oshihara, Appl. Catal. A. 200 (2000) 135.
[10] T. Ushikubo, H. Nakamura, Y. Koyasu, US Patent 5,380,933 (1995).
[11] M.M. Lin, M. Linsen, EP Patent 962,253A2 (1999).
[12] T. Ushikubo, Y. Koyasu, H. Nakamura, JP Patent 98,045,664 (1998).
[13] M. Takahashi, S. To, S. Hirose, JP Patent 98,120,617 (1998).
[14] W. Li, K. Oshihara, W. Ueda, Appl. Catal. A. 182 (1999) 357.
[15] J.N. Michaels, D.L. Stern, R.K. Grasselli, Catal. Lett. 42 (1996) 135.
[16] A. Laachir, V. Perrichon, A. Badri, J. Chem. Soc., Faraday Trans. 87 (10) (1991) 1601.
[17] F.L. Normand, L. Hilaire, K. Kili, J. Phys. Chem. 92 (1988) 2561.
[18] Y. Han, H. Wang, H. Cheng, J. Chem. Soc., Chem. Commun. (1999) 521.
[19] Y. Han, H. Wang, H. Cheng, R. Lin, J. Deng, New J. Chem. (1998) 1175.
[20] H. Cheng, Y. Han, H. Wang, Petrochem. Tech. 28 (1999) 803.
[21] Z. Wang, W. Wei, G. Liu, Acta Petrol. Sinica. 14 (1998) 21.
[22] A. Parmaliana, F. Arena, F. Frusteri, Stud. Surf. Sci. Catal. 110 (1997) 347.
[23] F. Arena, A. Parmaliana, J. Phys. Chem. 100 (1996) 19995.
[24] A. Laachir, V. Perrichon, A. Badri, J. Chem. Soc., Faraday. Trans. 87 (10) (1991) 1601.
[25] W. Wang, H.B. Zhang, G.D. Lin, Appl. Catal. B. 24 (2000) 219.
[26] M.C. Abello, M.F. Gomez, L.E. Cadus, Catal. Lett. 53 (1998) 185.
[27] K.M. Sancier, T. Dozono, H. Wise, J. Catal. 123 (1971) 270.
[28] K.M. Sancier, T. Dozono, H. Wise, J. Catal. 23 (1) (1971) 270.
[29] J. Soria, A. Martinez-Arias, J.C. Conesa, J. Chem. Soc., Trans. Faraday 9 (11) (1995) 1669.
[30] J. Barrault, C. Batiot, L. Magaud, Stud. Surf. Sci. Catal. 110 (1997) 375.
[31] P. Courtine, E. Bordes, Stud. Surf. Sci. Catal. 110 (1997) 177.
[32] H.B. Chen, D.W. Liao, L.J. Yu, et al., Appl. Surf. Sci. 147 (1–4) (1999) 85.
[33] L.B. Feng, H.Q. Wang, in: Y.G. Yin (Ed.), Characterization of Heterogeneous Catalysts, Chemical Engineering Press, Beijing, 1988, p. 487.
[34] A. Cervasini, A. Auroux, J. Catal. 131 (1991) 190.
[35] R. Grabowski, B. Grzybowska, K. Samson, Appl. Catal. A 125 (1995) 129.